## scientific reports



### **OPEN**

# Lamina cribrosa morphology and clinical implications in glaucoma with thin central corneal thickness

Sang Muk Lee<sup>1,2</sup>, Min Seon Park<sup>1,2</sup>, Garam Shin<sup>1,2</sup> & Sung Uk Baek<sup>1,2⊠</sup>

This study investigated the relationship between thin central corneal thickness (CCT) and lamina cribrosa (LC) morphology in patients with normal-tension glaucoma. Thin CCT was defined as a corneal thickness of less than 500 µm in both eyes, and all included patients had a corrected intraocular pressure of less than 20 mmHg. To investigate the LC-morphological characteristics observed in the *Thin-CCT group* (N = 60), the *Normal-CCT group* (N = 36) was set as the control. A subgroup analysis was performed on *Progressors* and *Non-progressors* using the visual field's progression rate to identify progression-related risk factors. The LC posterior displacement index was higher in the *Thin-CCT group* and the temporal anterior laminar insertion depth (ALID) was deeper in *Progressors*. In multivariate analyses, the risk of glaucoma progression increased with older age, thinner CCT, worse visual filed, deeper temporal ALID, and deeper mean LC depth. Notably, ALID showed a significant correlation with CCT. These findings suggest that in patients with normal-tension glaucoma, thinner CCT is associated with a more pronounced posterior displacement and deeper insertion of the LC, even under similar intraocular pressure conditions. The altered LC morphology observed in thin CCT may help explain the higher rate of glaucoma progression in this patient population.

**Keywords** Central corneal thickness, Lamina cribrosa, Posterior displacement index, Anterior laminar insertion depth

Thinner central corneal thickness (CCT) has been identified as a risk factor for the conversion of ocular hypertension to primary open-angle glaucoma (POAG), as well as for disease progression across various types of glaucoma <sup>1,2</sup>. Several mechanisms have been proposed to explain this association. One explanation is that thinner corneas may lead to underestimation of intraocular pressure (IOP) during measurement<sup>3,4</sup>. Another suggests that a thin cornea may be linked to increased biomechanical vulnerability of the optic nerve head (ONH) at a given IOP<sup>5,6</sup>.

Glaucomatous damage to the ONH involves multifactorial mechanisms, biomechanical factors playing a critical role in retinal ganglion cell injury. In this context, the cornea, an ocular structure with notable biomechanical properties, has been studied for its potential influence on ONH susceptibility. Both corneal hysteresis (CH) and CCT have been associated with the biomechanical response of the ONH to IOP. Since the lamina cribrosa (LC) is a primary site of glaucomatous axonal damage, a potential link between thin CCT and alterations in LC morphology has been proposed<sup>5,8,9</sup>.

Emerging evidence suggests that individuals with thin CCT may exhibit structural changes in the LC, such as increased curvature or thinning, which could enhance susceptibility to deformation<sup>9,10</sup>. These morphological alterations are believed to contribute to the pathogenesis of glaucoma. Therefore, understanding the relationship between CCT and LC morphology may provide valuable insights into disease mechanisms.

In this study, we investigated LC morphology in normal-tension glaucoma (NTG) patients with thin CCT, a group in which the influence of IOP on disease development is thought to be less dominant. Additionally, we examined the association between LC-structural characteristics and glaucoma progression within this population.

#### Results

#### Comparison between thin-CCT and normal-CCT groups

A total of 60 participants included as *Thin-CCT group* were selected at a 2:1 ratio with 36 *Normal-CCT group* matched for age, sex, and baseline severity of glaucoma. The baseline characteristics of the two groups are

<sup>1</sup>Department of Ophthalmology, Hallym University College of Medicine, Anyang, Korea. <sup>2</sup>Department of Ophthalmology, Hallym University Sacred Heart Hospital, 22, Gwanpyeong-ro, 170beon-gil, Dongan-gu, Anyang-si 14068, Gyeonggi-do, South Korea. <sup>∞</sup>email: postharuto@hanmail.net

Characteristics	Thin-CCT group 60 eyes	Normal-CCT group 36 eyes	P-value	
Age (years)	67.5 ± 13.5	63.0 ± 11.2	0.121	
Gender, male: female	1:1.61	1:1.60	0.485	
Diabetes mellitus, n (%)	14 (23.3)	10 (27.7)	0.546	
Hypertension, n (%)	22 (36.6)	13 (36.3)	0.340	
Central corneal thickness (µm)	483.50 ± 15.98	552.47 ± 19.24	< 0.001	
Spherical equivalent (diopter)	- 0.74 ± 1.80	- 2.06 ± 2.71	0.005	
Axial length (mm)	23.85 ± 0.84	24.49 ± 0.95	0.001	
Duration of follow-up (years)	4.51 ± 2.84	5.11 ± 2.02	0.260	
Phakia:Pseudophakia (n)	41:19	26:10	0.085	
Baseline IOP (mmHg)	13.70 ± 2.76	14.91 ± 2.54	0.334	
Corrected baseline IOP*(mmHg)	15.84 ± 2.57	14.54 ± 2.60	0.225	
Treated IOP (mmHg)	12.75 ± 2.09	13.3 ± 0.70	0.322	
Reduction rate of Treated IOP (%)	12.01%	9.49%	0.271	
Corrected treated-IOP*(mmHg)	14.77 ± 2.11	12.95 ± 2.01	0.136	
BCVA at baseline (Snellen)	0.86±0.19	0.94±0.14	0.189	
Initial MD (dB)	- 7.76 ± 6.50	- 6.36 ± 5.29	0.266	
Initial PSD (dB)	6.69 ± 4.24	6.60 ± 2.97	0.851	
Initial visual field index (%)	80.75 ± 21.35	93.10 ± 8.05	0.384	
Last MD (dB)	- 10.26 ± 8.31	- 6.86 ± 5.68	0.017	
Last PSD (dB)	7.12 ± 4.29	6.95 ± 4.77	0.826	
Last visual field index (%)	70.16 ± 28.16	81.63 ± 16.53	0.020	

**Table 1.** Comparison of clinical characteristics between *Thin-CCT group* and *Normal-CCT group*. The numbers in bold denote that the association is statistically significant (p < 0.05). *BCVA* best-corrected visual acuity, *MD* mean deviation, *PSD* pattern standard deviation. \*IOP – (CCT-545)/50×2.5.

				Thin-CCT group		
Lamina cribrosa	Thin-CCT group 60 eyes	Normal-CCT group 36 eyes	P-value	Progressors 28 eyes	Non-progressors 32 eyes	P-value
BMO distance (µm)	1886.3 ± 231.8	1813.9 ± 183.8	0.102	1847.0 ± 246.4	1925.5 ± 215.4	0.245
LC thickness (µm)	228.2 ± 29.5	240.0 ± 33.6	0.353	221.1 ± 28.5	236.2 ± 30.9	0.437
Nasal ALID (μm)	267.5 ± 94.1	250.1 ± 88.9	0.117	275.1 ± 104.1	259.8 ± 90.6	0.248
Temporal ALID (μm)	299.4 ± 86.1	278.5 ± 78.1	0.703	316.5 ± 93.8	280.3 ± 80.7	0.048
Average ALID (µm)	283.4 ± 82.0	264.3 ± 74.4	0.285	295.5 ± 87.2	269.8 ± 84.3	0.094
Mean LC depth	669.6 ± 145.4	608.2 ± 137.4	0.204	675.7 ± 146.3	658.6 ± 139.4	0.568
LC posterior displacement index	626.2 ± 181.0	533.9 ± 160.3	0.034	622.8 ± 168.9	630.1 ± 171.5	0.912

**Table 2**. Comparison of lamina cribrosa morphology among subgroups. The numbers in bold denote that the association is statistically significant (p < 0.05). BMO Bruch's membrane opening, ALID anterior laminar insertion depth, LC lamina cribrosa.

summarized in Table 1. As expected, there was an average CCT difference of about 70  $\mu$ m between the *Thin-CCT group* (483.50  $\pm$  15.98  $\mu$ m) and the *Normal-CCT group* (552.47  $\pm$  19.24  $\mu$ m) (P<0.001) (Table 1).

The interobserver agreements for measuring LC parameters of 30 patients (20 *Thin-CCT group* and 10 *Normal-CCT group* patients) were excellent, with an intra-class correlation coefficient (ICC) for Bruch's membrane opening (BMO) distance of 0.902 (0.842–0.945), an ICC for temporal anterior laminar insertion depth (ALID) of 0.894 (0.846–0.932), an ICC for nasal ALID of 0.805 (0.719–0.874) and an ICC for LC thickness of 0.895 (0.834–0.940). In the optical coherent tomography (OCT)-based morphological analysis of the LC between the *Thin-CCT group* and the *Normal-CCT group*, there was no difference in LC thickness (P = 0.353, Table 2). However, the LC posterior displacement index was significantly higher in the *Thin-CCT group*, suggesting greater posterior bowing of LC curvature (P = 0.034).

#### Multivariate logistic regression and correlation analyses

Univariate and multivariate logistic regression analyses employing a forward conditional method were performed to determine the factors associated with progression of glaucoma (Table 3). In the multivariate logistic analyses, the risk of glaucoma progression increased with older age (hazard ratio [HR] 1.071, P=0.007), thinner CCT (HR 0.988, P=0.010) worse initial MD value (HR 0.863, P=0.005), deeper temporal ALID (HR 1.009, P=0.002), and

	Univariate			Multivariate			
	Hazard ratio	Confidence interval (95%)	P value	Hazard ratio	Confidence interval (95%)	P-value	
Age (years)	1.052	1.014-1.091	0.007	1.071	1.019-1.125	0.007	
Gender, female	0.888	0.382-2.063	0.782				
Diabetes mellitus, n (%)	1.001	0.904-1.069	0.951				
Hypertension, n (%)	0.763	0.606-1.069	0.082				
Central corneal thickness (µm)	0.985	0.973-0.996	0.009	0.988	0.962-0.998	0.010	
Spherical equivalent (diopter)	1.057	0.878-1.272	0.559				
Axial length (mm)	1.475	0.859-2.355	0.152				
Duration of follow-up (years)	1.210	1.021-1.434	0.028	1.267	0.985-1.629	0.065	
Lens status, pseudophakia	2.496	0.960-6.491	0.061				
Baseline IOP (mmHg)	1.056	0.907-1.230	0.481				
Corrected baseline IOP*(mmHg)	1.119	0.962-1.302	0.146				
Treated IOP with topical medication	0.979	0.802-1.194	0.831				
Reduction rate of treated IOP (%)	2.602	1.044-6.488	0.040				
Corrected treated-IOP*(mmHg)	1.180	0.976-1.180	0.087				
BCVA at baseline (Snellen)	0.186	0.018-1.874	0.153				
Initial MD (dB)	0.854	0.783-0.931	< 0.001	0.863	0.781-0.956	0.005	
Initial PSD (dB)	1.141	1.031-1.263	0.011				
BMO distance (µm)	0.999	0.997-1.001	0.438				
LC thickness (µm)	0.998	0.993-1.002	0.307				
Nasal ALID (µm)	1.001	0.999-1.004	0.401				
Temporal ALID (μm)	1.003	1.000-1.006	0.031	1.009	1.003-1.015	0.002	
Average ALID (µm)	1.002	1.000-1.005	0.102				
Mean LC depth	1.006	1.002-1.011	0.017	1.007	1.003-1.008	0.025	
LC posterior displacement index	1.000	0.998-1.002	0.997				

**Table 3**. Univariate and multivariate logistic regression analyses of parameters associated with glaucoma progression in NTG patients. Variables with P < 0.05 in the univariate analysis (age, CCT, duration of follow-up, initial MD, temporal ALID, and mean LC depth) were included in the multivariate model to identify independent predictors. BMO Bruch's membrane opening, ALID anterior laminar insertion depth, LC lamina cribrosa. The numbers in bold denote that the association is statistically significant (p < 0.05).

Independent variables	LC-morphological parameters	R <sup>2</sup>	Coefficient	Constant	VIF	P-value
ССТ (µm)	BMO (μm)	0.089	- 1.262	2502.7	1.000	0.065
	LC thickness (μm)	0.128	0.247	52.3	1.756	0.182
	Nasal ALID (µm)	0.143	0.385	320.0	1.082	0.020
	Temporal ALID (μm)	0.177	0.409	384.2	1.113	0.001
	Mean LC depth (μm)	0.091	0.204	383.9	1.784	0.175
	LC posterior displacement index	0.076	- 0.487	180.6	1.331	0.238

**Table 4.** Multiple linear regression analysis assessing the association between CCT and LC morphology, as adjusted for axial length and spherical equivalent. CCT central corneal thickness, BMO Bruch's membrane opening, ALID anterior laminar insertion depth, LC lamina cribrosa, VIF variance inflation factor. Bold values indicate statistically significant associations (p < 0.05).

deeper mean LC depth (HR 1.007, P=0.025). A correlation analysis was then performed to find LC parameters associated with CCT, which had been identified as a risk factor for glaucoma progression (Table 4). Among the several indicators, ALID showed a significant correlation with CCT (nasal ALID:  $R^2$ =0.143, P=0.020; temporal ALID:  $R^2$ =0.177, P=0.001).

#### Comparison between progressors and non-progressors in Thin-CCT group

Specifically, to identify risk factors for glaucoma progression among the *Thin-CCT group*, a subgroup analysis was performed by dividing into *Progressors* and *Non-progressors* (Online eTable 1). The *Progressors* were older than the *Non-progressors* (P=0.011) and initial MD, PSD, and visual field index (VFI) were worse in the *Progressors* (all P<0.001). However, there was no significant difference in most of the LC parameters between the *Progressors* and *Non-progressors* (Table 2). Only temporal ALID was deeper in the *Progressors* (316.5 $\pm$ 93.8 vs. 280.3 $\pm$ 80.7 µm, P=0.048).

#### Discussion

The aim of the present study was to determine whether NTG patients with thin CCT exhibit different LC morphology compared with those with normal CCT. To our knowledge, this is the first study to evaluate the LC for a specific group, such as, in the current case, NTG with thin CCT. NTG patients pose a unique challenge in glaucoma management, due to NTG's association with normal or low IOP levels despite progressive optic nerve damage. In addition, thin CCT is well known as a potent risk factor for progression of glaucoma. In this respect, understanding the structural characteristics of LC in NTG patients with thin CCT could provide insight into the pathophysiology of disease progression.

There was no difference in LC thickness between the *Thin-CCT* and *Normal-CCT groups*. Additionally, similarly to previous studies<sup>11,12</sup>, our findings showed that CCT did not show any correlation with LC thickness. Lee et al. <sup>12</sup> analyzed the association among axial length, CCT, and LC thickness in healthy subjects, and reported that neither CCT nor axial length was significantly associated with central LC thickness. In this study, we examined not only the thickness of the LC but also its depth and posterior displacement index. Our results demonstrated that the *Thin-CCT group* exhibited a significantly higher LC posterior displacement index. Furthermore, a thinner CCT was associated with deeper LC insertion. These findings suggest that NTG patients with thinner CCT may experience a greater degree of posterior LC bowing. Taken together, these observations imply that increased LC posterior displacement in eyes with thin CCT may be more closely related to the biomechanical properties, such as stiffness and elasticity of the LC, rather than to its thickness alone.

Importantly, no differences were observed in baseline or treated IOP, corrected for CCT, between the *Thin-CCT* and *Normal-CCT groups*. Although this study did not perform a detailed comparison with IOP-matched controls, the mechanical load exerted on the LC can be assumed to be similar across groups. Despite this similarity in IOP, the degree of posterior LC deformation was significantly greater in the *Thin-CCT group*. This finding further supports the notion that structural susceptibility of the LC, rather than pressure load alone, may contribute to LC deformation in eyes with thinner corneas.

Posterior LC displacement is a well-documented phenomenon in glaucomatous eyes and is considered a key pathogenic event contributing to optic nerve damage. This displacement can disrupt axoplasmic flow by kinking or compressing retinal ganglion cell axons as they pass through the LC, thereby leading to glaucomatous damage<sup>13</sup>. In previous studies, LC posterior displacement was highly correlated with progression of glaucoma<sup>14</sup>, and its position changed according to IOP<sup>15</sup>. Taken together, our findings may help explain the higher rate of glaucoma progression observed in patients with thin CCT, specifically by highlighting the role of LC morphology and biomechanics in disease pathogenesis.

The exact mechanism underlying more pronounced posterior LC displacement in eyes with thin CCT remains unclear but may be inferred from prior research. Previous studies have demonstrated that lower CH, a marker of corneal biomechanical integrity, is associated with progressive posterior displacement of the anterior LC<sup>9</sup>. Lee et al.<sup>5</sup> further reported that lower CH was correlated with increased LC curvature in POAG patients. Given the strong correlation between CH and CCT<sup>16</sup>, the observed association in our study between thin CCT and pronounced LC deformation may reflect this biomechanical link. However, Lee et al. did not find any direct correlation between CCT and LC curvature, possibly due to differences in their study populations. Their study included subjects with normal CCT, whereas ours focused exclusively on NTG patients with thin CCT. Further research incorporating CH and corneal resistance factor in thin-CCT populations is warranted in order to clarify whether CCT independently influences LC morphology or acts through related biomechanical properties.

In this study, although nasal ALID did not show a significant association, temporal ALID was significantly deeper in *Progressors* within the *Thin-CCT group*. One possible explanation for this finding can be drawn from a study by Lee et al. <sup>17</sup>, which reported that ALID is more posteriorly located in patients with POAG relative to normal controls, with notable regional variations. Specifically, posterior insertion was observed in the inferotemporal (6–7 o'clock), superotemporal (9.5–12 o'clock), and nasal (2.5–3 o'clock) meridians. These findings suggest regional variability in ALID across different sectors of the LC, likely reflecting localized susceptibility to IOP-induced stress. Notably, POAG eyes demonstrated regional differences in LC morphology that corresponded to the locations of retinal nerve fiber layer (RNFL) defects <sup>18</sup>. The temporal region, in particular, is a common site of glaucomatous damage and may be more susceptible to posterior displacement of the LC. Our findings support this notion, suggesting that temporal ALID changes may be more closely associated with disease progression, especially in patients with thin CCT.

Although the difference was not statistically significant, the *Thin-CCT group* was older than the *Normal-CCT group* (67.5 vs. 63.0 years), and age was identified as a significant risk factor for glaucoma progression (HR = 1.071). Age-related structural changes, such as LC sclerosis, can contribute to LC deformation<sup>19</sup>. Moreover, as CCT tends to decrease with age<sup>20</sup>, the observed association between thin CCT and LC morphology in this study may have been confounded by age. Therefore, future studies should incorporate age-stratified analyses to better clarify the independent impact of thin CCT on LC-structural characteristics.

In the subgroup analysis of the *Thin-CCT group*, *Progressors* were older and exhibited more severe initial glaucoma findings compared to *Non-progressors*, both well-established risk factors for disease progression<sup>21</sup>. Interestingly, most LC parameters did not differ significantly between the two subgroups, with the exception of deeper ALID in the *Progressors*. This suggests that among patients with thin CCT and similar LC morphology, age and baseline disease severity may exert additional influence on glaucoma progression, reinforcing their known prognostic relevance.

Our study has some limitations. First, only horizontal scans of the ONH were analyzed during the LC analysis in this study. The authors consider that measuring vertical and radial scans together and selecting the average value will help increase accuracy. Future research to improve this limitation will be necessary. Second, this study did not include a comparison with healthy subjects. Both the study and control groups consisted solely of NTG patients, all of whom may have already exhibited LC deformation, such as thinning and posterior

displacement, due to glaucomatous damage. As a result, intergroup differences in LC morphology may have been underestimated. Future studies including healthy controls are warranted in order to more clearly delineate the biomechanical association between thin CCT and LC deformation. Lastly, peripapillary sclera and choroidal thickness were not investigated in this study. The thickness of the sclera and choroid around the LC may be a confounding factor and may be an important link for pathogenesis.

In conclusion, our study revealed that NTG patients with thin CCT exhibited differences in the structure of the LC. These findings could contribute to the growing body of evidence suggesting that corneal thickness may be associated with LC morphology. Furthermore, understanding these relationships can help in the development of more accurate diagnostic and management strategies for thin CCT patients.

#### Methods

#### Ethics

All the subjects had been consecutively enrolled at the Glaucoma Clinic of Hallym Sacred Heart Hospital between 2018 and 2022. This study was conducted in compliance with the Declaration of Helsinki and was approved by the Institutional Review Board of Hallym Sacred Heart Hospital (IRB approval number: 2021-08-007). Due to the retrospective nature of the study, the Institutional Review Board of Hallym University Sacred Heart Hospital waived the need of obtaining informed consent.

#### Study subjects

All of the enrolled patients were diagnosed with NTG, defined as unilateral or bilateral glaucomatous optic disc cupping and corresponding visual field defects, with pre-treatment IOP (corrected for CCT) consistently below 20 mmHg in at least two baseline measurements<sup>3,22</sup>. All patients also had a minimum of three years of follow-up to monitor glaucoma progression.

The subjects additionally met the following further criteria for study inclusion: (1) age > 18 years; (2) open angle confirmed by gonioscopic examination; (3) best-corrected visual acuity (BCVA) of 20/40 or better; (4) refraction within  $\pm$  6.0 diopters spherical and within  $\pm$  3.0-diopters cylinder at study. The exclusion criteria were as follows: (1) history of surgery or corneal disease affecting corneal thickness; (2) history of ocular surgery (other than uncomplicated cataract extraction more than 6 months previous to enrollment); (3) any history of retinal pathology or non-glaucomatous optic neuropathy; (4) history of ocular trauma, uveitis, acute or intermittent angle-closure attack; (5) OCT scans with poor demarcation of the peripheral LC due to focal LC defects or vascular shadowing. Only one eye per patient was included, and if both eyes met the eligibility criteria, one eye was randomly selected.

#### Central cornea thickness and corrected intraocular pressure

In this study, thin CCT was defined as less than 500  $\mu m$  in both eyes. This value was based on the average CCT for various countries and ethnicities, which ranges from approximately 520 to 540  $\mu m$  (standard deviation 30  $\mu m$ )<sup>23,24</sup>, as well as a Korean NTG study in which average CCT was 537.5±33.0  $\mu m^{25}$ . Among the total NTG cohort, *Normal-CCT group* was formed for control and comparative analysis purposes. The *Normal-CCT group* criteria were both CCT  $\geq$ 530  $\mu m$  and, to exclude thick corneas, < 600  $\mu m^2$ . Patients with CCT values between 500 and 529  $\mu m$  were excluded to preserve a meaningful distinction between the groups and avoid dilution of the observed effects related to CCT differences.

CCT was recorded as the average value based on 50 meridional sections photographed from the center of the cornea using Pentacam\* HR (Oculus, Wetzlar, Germany). We adopted and analyzed both IOP as measured by Goldmann tonometry and IOP as corrected for CCT. In this study, IOP corrected for CCT was calculated using the following formula<sup>23</sup>: "Corrected IOP = IOP - (CCT-545)/50  $\times$  2.5".

#### Control and subgroup analyses

All of the subjects in the *Thin-CCT group* who met the inclusion criteria during the study period were initially enrolled, and the final study population was determined after applying the exclusion criteria. A control group with normal CCT (*Normal-CCT group*) was subsequently matched to the *Thin-CCT group* at a 2:1 ratio based on age, sex, and baseline glaucoma severity. During this process, the minimum number of control subjects for statistical power was maintained.

To identify risk factors associated with glaucoma progression, the *Thin-CCT group* was further stratified into two subgroups: *Progressors* and *Non-progressors*. This classification was based on trend-based analysis using the Guided Progression Analysis software. Patients with a MD slope of less than -1.0 dB/year were classified as *Progressors*, while those with an MD slope of -1.0 dB/year or greater were classified as *Non-progressors*<sup>26,27</sup>.

#### Ophthalmologic examinations

All of the subjects underwent detailed ophthalmologic examinations, including baseline IOP measurement by Goldman applanation tonometry (Haag-Streit), anterior chamber angle measurement by gonioscopy, BCVA, determination of the refractive value with an autorefractor (HRK-8000 A, Huvitz, Gunpo, Korea), and a dilated fundus examination. After pupil dilation, all of the subjects were imaged by optic disc photography and red-free fundus photography (Vx-10; Kowa Optimed Inc., Tokyo, Japan). Axial length was measured by optical biometry, and RNFL thickness by OCT. All also underwent standard automated perimetry using the Swedish interactive threshold algorithm with the 24-2 or 30-2 standard program (Humphrey Field Analyzer II; Carl Zeiss Meditec Inc., Dublin, CA, USA).

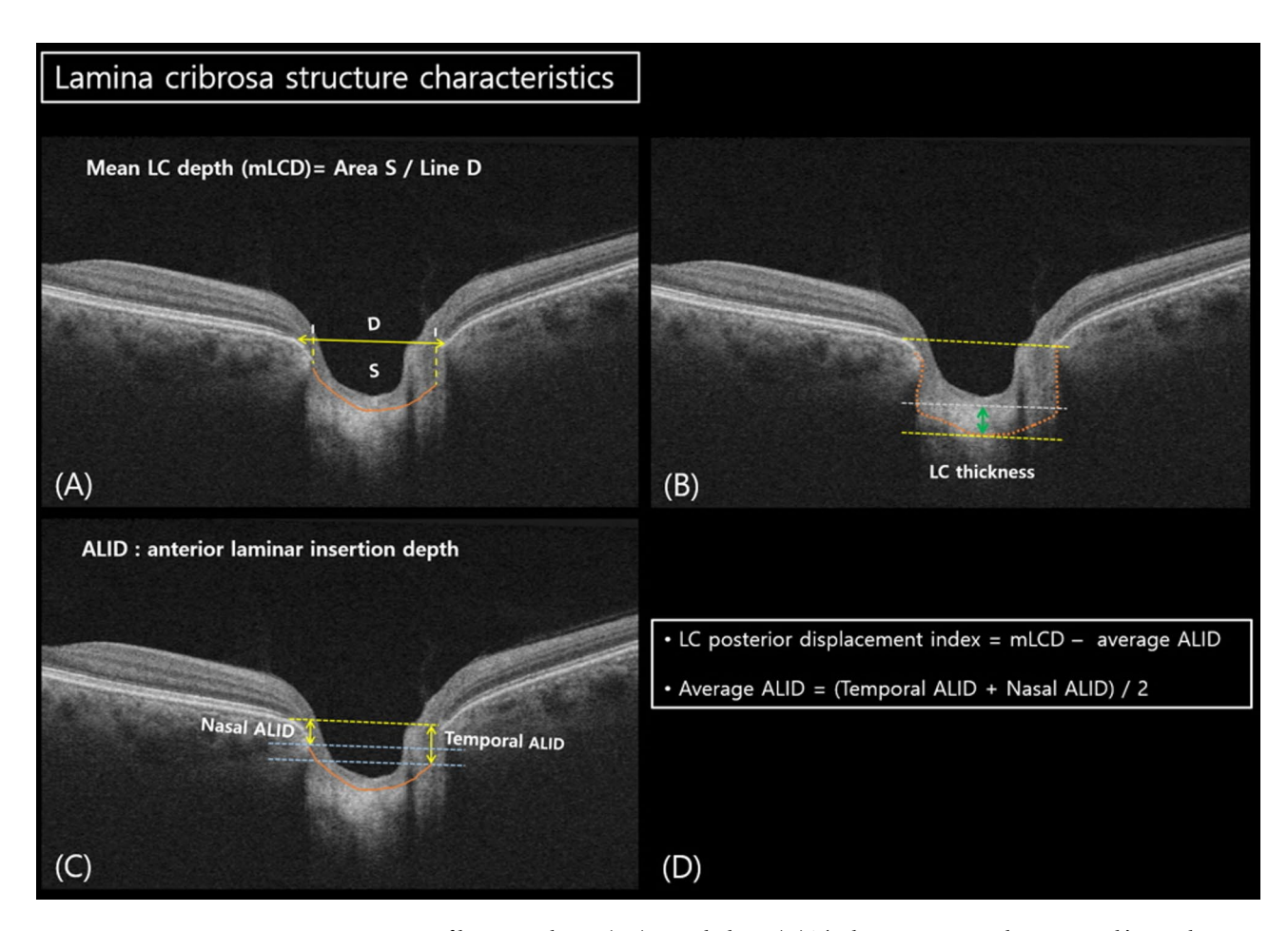


Fig. 1. Assessment of lamina cribrosa (LC) morphology. (A) The line connecting the two Bruch's membrane openings (BMO) is selected as the reference plane. The anterior LC surface is manually depicted as an orange-color line. Connect each end of the orange-color line perpendicularly to the BMO connecting line (yellow dashed line). The distance between two intersection points is defined as 'Line D'. The space surrounded by 'Line D', yellow-dotted line, and the border of the anterior LC surface was defined as 'Area S'. The mean LC depth (mLCD) was computed by dividing 'Area S' by 'Line D'. (B) LC thickness was defined as the perpendicular distance between the internal limiting membrane surface and the posterior laminar surface. The distance from the maximally depressed point (grey dashed line) of the optic nerve surface to the level of the posterior border of the LC was measured and adopted (green arrow). (C) The two vertical lines are drawn from the anterior laminar insertion (ALI) to the BMO reference plane. The two blue-dotted lines are drawn parallel to the BMO reference plane at each ALI. The cross points indicate the extent of the anterior laminar insertion depth (ALID). (D) The LC posterior displacement index represent the difference between the mLCD and the ALID (mLCD – ALID). The average ALID was calculated from the mean values of the nasal and temporal ALIDs.

#### Swept-source optical coherence tomography imaging of lamina cribrosa

LC morphology was analyzed using OCT scans measured prior to anti-glaucoma medication treatment. All of the subjects had been scanned with the DRI Swept-Source Optical Coherence Tomography (SS-OCT) device (Topcon Medical Systems, Oakland, NJ, USA). One horizontal cross-scan, centered at the ONH and 6.0-mm in width, was performed. The center of the ONH was identified where the trunk of the central vessels came out from the ONH, and two observers (S.M.L., S.U.B.) measured right at the temporal side of the trunk of the central vessels. Adjustment of contrast and brightness settings aided in identifying images that provided the clearest visualization of LC morphology<sup>28</sup>. Only qualified images, which is to say, those with a signal strength of  $\geq 60 \ (100 = \text{maximum})$  without segmentation failure, motion artifacts, or decentration of the measurement circle, were included. All of the OCT measurements were performed using ImageJ software (available at http://imagej.nih.gov/ij/).

#### Structural assessment of lamina cribrosa parameters

The BMO was defined as the termination of the Bruch's membrane (one point on each side of the B-scan), and the line connecting both ends of the Bruch's membrane was defined as the BMO distance (Fig. 1A)<sup>29–31</sup>. The LC was identified as a highly reflective plate-like structure after adjusting of image brightness and contrast. The anterior LC surface was manually demarcated as if there was no discontinuity in the anterior LC border, including LC pores or vascular shadowing<sup>30</sup>.

The LC thickness was defined as the vertical distance between the internal limiting membrane surface and the posterior laminar surface (Fig. 1B)<sup>32</sup>. For this measurement, the distance from the maximally depressed point of the optic nerve surface to the level of the posterior border of the LC was measured. The borders of the LC were considered to be where the highly reflective region started and finished, which corresponded with the hyporreflective columns through which the axons run. Meanwhile, two vertical lines were drawn from the anterior laminar insertion (ALI) to the BMO reference plane. Two blue-dotted lines were then drawn parallel to the BMO reference plane to each ALI, which lines indicated the extent of ALID. The mean values of temporal and nasal ALID were defined as the average ALID (Fig. 1C,D)<sup>17,33</sup>.

The examiner measured the area enclosed by the anterior laminar surface, the two vertical lines for the ALID measurement, and the BMO reference plane. The mean LC depth (mLCD) was computed by dividing this area (Area S) by the length between the two cross-points made by vertical lines drawn from the ALI to the BMO reference plane (Line D) (Fig. 1A). LC posterior displacement index measurements were calculated as the difference between the mLCD and the ALID (mLCD-ALID) (Fig. 1D). Therefore, a higher LC posterior displacement index suggested more posterior bending of the LC<sup>31,34</sup>.

All of the SS-OCT images were taken by one experienced technician. All were analyzed by two ophthalmologists (S.M.L, S.U.B.) masked to the subjects' clinical information. The intra-observer and inter-observer reproducibility of the ONH were evaluated by reference to 15 randomly selected OCT B-scans from 15 eyes. The absolute agreement of a single observer's measurements and the average of the measurements performed by the 2 observers were calculated using the ICC via a two-way mixed-effect model.

#### Statistical analysis

The interobserver agreement on the measuring of the LC parameters was evaluated by calculating 95% ICCs using OCT scans of 30 randomly selected eyes. The ICC values ranged from 0 to 1, with a higher value indicating better reliability. ICCs < 0.40 were considered poor, those between 0.4 and 0.6 fair, those between 0.61 and 0.8 good, and those greater than 0.8 excellent<sup>35</sup>.

The comparison between subgroups used the independent t-test for continuous variables and the  $\chi^2$  test for categorical variables. Univariate and multivariate logistic regression analyses employing a forward conditional method were performed to determine the associations of individual factors with progression of glaucoma; HRs and 95% confidence intervals were recorded. To avoid multi-collinearity, variables correlating significantly with each other were not assessed simultaneously. Instead, the variable with the highest significance among correlated variables was adopted. Regression analyses examining the relationship between CCT and LC morphology were adjusted for axial length and spherical equivalent in order to control for their potential confounding effects.

All of the statistical analyses were performed using SPSS version 21.0 (SPSS, Chicago, IL, USA). All of the P-values were two-sided and were considered significant when < 0.05.

#### Data availability

Data supporting the findings of the current study are available from the corresponding author on reasonable request.

Received: 29 October 2024; Accepted: 5 June 2025

Published online: 01 July 2025

#### References

- 1. Brandt, J. D., Beiser, J. A., Kass, M. A., Gordon, M. O. & Group, O. H. T. S. Central corneal thickness in the ocular hypertension treatment study (OHTS). *Ophthalmology* 108 (10), 1779–1788 (2001).
- 2. Gordon, M. O. et al. The ocular hypertension treatment study: baseline factors that predict the onset of primary open-angle glaucoma. *Arch. Ophthalmol.* **120** (6), 714–720 (2002).
- 3. Ehlers, N., Bramsen, T. & Sperling, S. Applanation tonometry and central corneal thickness. *Acta Ophthalmol.* **53** (1), 34–43 (1975).
- 4. Sng, C., Barton, K., Kim, H., Yuan, S. & Budenz, D. L. Central corneal thickness and its associations with ocular and systemic factors in an urban West African population. *Am. J. Ophthalmol.* **169**, 268–275 (2016).
- 5. Lee, K. M. et al. Association of corneal hysteresis with lamina cribrosa curvature in primary open angle glaucoma. *Investig. Ophthalmol. Vis. Sci.* 60 (13), 4171–4177 (2019).
- 6. Matsuura, M. et al. Relationship between novel intraocular pressure measurement from Corvis ST and central corneal thickness and corneal hysteresis. *Br. J. Ophthalmol.* **104** (4), 563–568 (2020).
- 7. Burgoyne, C. F. A Biomechanical paradigm for axonal insult within the optic nerve head in aging and glaucoma. Exp. Eye Res. 93 (2), 120–132 (2011).
- 8. Park, K., Shin, J. & Lee, J. Relationship between corneal Biomechanical properties and structural biomarkers in patients with normal-tension glaucoma: a retrospective study. *BMC Ophthalmol.* **18**, 1–10 (2018).
- 9. Wong, B. J. et al. Relationship of corneal hysteresis and anterior lamina cribrosa displacement in glaucoma. *Am. J. Ophthalmol.* 212, 134–143 (2020).
- 10. Akkaya, S. & Küçük, B. Lamina cribrosa thickness in patients with keratoconus. Cornea 36 (12), 1509-1513 (2017)
- 11. Jonas, J. B. & Holbach, L. Central corneal thickness and thickness of the lamina cribrosa in human eyes. *Investig. Ophthalmol. Vis. Sci.* 46 (4), 1275–1279 (2005).
- 12. Lee, E. J., Kim, T-W., Weinreb, R. N., Suh, M. H. & Kim, H. Lamina cribrosa thickness is not correlated with central corneal thickness or axial length in healthy eyes: central corneal thickness, axial length, and lamina cribrosa thickness. *Graefe's Archive Clin. Experimental Ophthalmol.* 251, 847–854 (2013).
- 13. Yan, D. et al. Deformation of the lamina cribrosa by elevated intraocular pressure. Br. J. Ophthalmol. 78 (8), 643-648 (1994).
- 14. Park, S. C. et al. Lamina cribrosa depth in different stages of glaucoma. Investig. Ophthalmol. Vis. Sci. 56 (3), 2059-2064 (2015).
- 15. Lee, E. J. & Kim, T-W. Lamina cribrosa reversal after trabeculectomy and the rate of progressive retinal nerve fiber layer thinning. *Ophthalmology* 122 (11), 2234–2242 (2015).
- Mangouritsas, G., Morphis, G., Mourtzoukos, S. & Feretis, E. Association between corneal hysteresis and central corneal thickness in glaucomatous and non-glaucomatous eyes. Acta Ophthalmol. 87 (8), 901–905 (2009).

- 17. Lee, K. M. et al. Anterior lamina cribrosa insertion in primary open-angle glaucoma patients and healthy subjects. *PLoS One.* **9** (12), e114935 (2014).
- 18. Kim, J-A., Kim, T-W., Lee, E. J., Girard, M. J. & Mari, J. M. Lamina cribrosa morphology in glaucomatous eyes with Hemifield defect in a Korean population. *Ophthalmology* 126 (5), 692–701 (2019).
- 19. Albon, J., Purslow, P. P., Karwatowski, W. S. & Easty, D. L. Age related compliance of the lamina cribrosa in human eyes. *Br. J. Ophthalmol.* 84 (3), 318–323 (2000).
- 20. Brandt, J. D. et al. Changes in central corneal thickness over time: the ocular hypertension treatment study. *Ophthalmology* **115** (9), 1550–1556 (2008). e1.
- 21. Leske, M. C. et al. Factors for glaucoma progression and the effect of treatment: the early manifest glaucoma trial. *Arch. Ophthalmol.* **121** (1), 48–56 (2003).
- Group, C. N. T. G. S. The effectiveness of intraocular pressure reduction in the treatment of normal-tension glaucoma. Am. J. Ophthalmol. 126 (4), 498–505 (1998).
- 23. Orssengo, G. J. & Pye, D. C. Determination of the true intraocular pressure and modulus of elasticity of the human cornea in vivo. *Bull. Math. Biol.* 61 (3), 551–572 (1999).
- 24. Belovay, G. W. & Goldberg, I. The Thick and thin of the central corneal Thickness in glaucoma. Eye 32 (5), 915-923 (2018).
- 25. Lee, E. S., Kim, C. Y., Ha, S. J., Seong, G. J. & Hong, Y. J. Central corneal thickness of Korean patients with glaucoma. *Ophthalmology* 114 (5), 927–930 (2007).
- 26. Peters, D., Bengtsson, B. & Heijl, A. Factors associated with lifetime risk of open-angle glaucoma blindness. *Acta Ophthalmol.* **92** (5), 421–425 (2014).
- 27. Liebmann, K., De Moraes, C. G. & Liebmann, J. M. Measuring rates of visual field progression in linear versus nonlinear scales: implications for Understanding the relationship between baseline damage and target rates of glaucoma progression. *J. Glaucoma*. 26 (8), 721–725 (2017).
- 28. Girard, M. J., Strouthidis, N. G., Ethier, C. R. & Mari, J. M. Shadow removal and contrast enhancement in optical coherence tomography images of the human optic nerve head. *Investig. Ophthalmol. Vis. Sci.* 52 (10), 7738–7748 (2011).
- 29. Moghimi, S. et al. Crowded optic nerve head evaluation with optical coherence tomography in anterior ischemic optic neuropathy. *Eye* **31** (8), 1191–1198 (2017).
- 30. Lee, E. J. et al. Visualization of the lamina cribrosa using enhanced depth imaging spectral-domain optical coherence tomography. *Am. J. Ophthalmol.* **152** (1), 87–95 (2011). e1.
- 31. Kim, Y. W. et al. Clinical assessment of lamina cribrosa curvature in eyes with primary open-angle glaucoma. *PloS One.* 11 (3), e0150260 (2016).
- 32. Lee, S. H., Kim, T-W., Lee, E. J., Girard, M. J. & Mari, J. M. Lamina cribrosa curvature in healthy Korean eyes. Sci. Rep. 9 (1), 1756 (2019).
- 33. Park, S. C. et al. Horizontal central ridge of the lamina cribrosa and regional differences in laminar insertion in healthy subjects. *Investig. Ophthalmol. Vis. Sci.* **53** (3), 1610–1616 (2012).
- 34. Ha, A. et al. Baseline lamina cribrosa curvature and subsequent visual field progression rate in primary open-angle glaucoma. *Ophthalmology* **125** (12), 1898–1906 (2018).
- 35. Landis, J. R. & Koch, G. G. The measurement of observer agreement for categorical data. Biometrics 159-174. (1977).

#### **Author contributions**

SML and SUB designed the study. SML, MSP, GS, and SUB collected the data. SML and SUB verified the data. SML and SUB did manual measurements of parameters and statistical analysis. SML, MSP, and SUB interpreted the data and wrote the first draft. All authors critically revised the manuscript and approved the final manuscript.

#### **Funding**

This research did not receive any specific grant from funding agencies in the public, commercial, or not-for-profit sectors.

#### **Declarations**

#### Competing interests

The authors declare no competing interests.

#### Additional information

**Supplementary Information** The online version contains supplementary material available at https://doi.org/10.1038/s41598-025-06069-8.

**Correspondence** and requests for materials should be addressed to S.U.B.

Reprints and permissions information is available at www.nature.com/reprints.

**Publisher's note** Springer Nature remains neutral with regard to jurisdictional claims in published maps and institutional affiliations.

**Open Access** This article is licensed under a Creative Commons Attribution-NonCommercial-NoDerivatives 4.0 International License, which permits any non-commercial use, sharing, distribution and reproduction in any medium or format, as long as you give appropriate credit to the original author(s) and the source, provide a link to the Creative Commons licence, and indicate if you modified the licensed material. You do not have permission under this licence to share adapted material derived from this article or parts of it. The images or other third party material in this article are included in the article's Creative Commons licence, unless indicated otherwise in a credit line to the material. If material is not included in the article's Creative Commons licence and your intended use is not permitted by statutory regulation or exceeds the permitted use, you will need to obtain permission directly from the copyright holder. To view a copy of this licence, visit <a href="https://creativecommons.org/licenses/by-nc-nd/4.0/">https://creativecommons.org/licenses/by-nc-nd/4.0/</a>.

© The Author(s) 2025